

# The Hierarchy of Stable Distributions and Operators to Trade Off Stability and Performance

Adarsh Subbaswamy  
Johns Hopkins University  
asubbaswamy@jhu.edu

Bryant Chen  
Brex\*  
bryant@brex.com

Suchi Saria  
Johns Hopkins University  
ssaria@cs.jhu.edu

## Abstract

Recent work addressing model reliability and generalization has resulted in a variety of methods that seek to proactively address differences between the training and unknown target environments. While most methods achieve this by finding distributions that will be invariant across environments, we will show they do not necessarily find the same distributions which has implications for performance. In this paper we unify existing work on prediction using stable distributions by relating environmental shifts to edges in the graph underlying a prediction problem, and characterize stable distributions as those which effectively remove these edges. We then quantify the effect of edge deletion on performance in the linear case and corroborate the findings in a simulated and real data experiment.

## 1 Introduction

Increasing deployment of machine learning models in high impact applications such as healthcare (Henry et al., 2015; Yu et al., 2018) and criminal justice (Lum and Isaac, 2016) has led to renewed emphasis on improving and ensuring their *safety* and *reliability* (Amodei et al., 2016; Saria and Subbaswamy, 2019). To do so, developers are forced to reason in advance about likely sources of failure and address them prior to deployment. One source of failure is due to *shifts in environment* between the environment in which training data was collected and the environment in which the model will be deployed. In cases where data from the deployment environment is unavailable, failing to account for the differences can result in dangerous decisions and worse performance than anticipated.

For example, Caruana et al. (2015) consider a case in which a model was trained to predict mortality ( $M$ ) due to pneumonia ( $P$ ) using data from hospitalized patients. The motivation of the original study (Cooper et al., 1997) was to deploy the model for triage—to determine whether to admit patients or treat them at home—representing a shift to a new environment in which the patients have not yet been hospitalized. In this case, the model learned an *unstable* association in the source environment that does not hold in the deployment environment: it learned that patients with asthma ( $A$ ) were less likely to die because of admission policy since asthmatic patients were more likely to be directly admitted to the ICU ( $I$ ) at the hospital. In the deployment environment the patients have not been admitted to the hospital (i.e., admission policy is different) and thus the model makes dangerously incorrect predictions that asthmatic patients have lower risk of mortality.

In recent work addressing such shifts in environment, Subbaswamy et al. (2019) provided a graphical language for expressing shifts that are likely to occur. They explicitly represent the underlying data generating process (DGP) with a graph of causal mechanisms (directional knowledge of causes and effects) relating the variables in a prediction problem. The graph is augmented to identify the pieces of the DGP (i.e., conditional distributions encoding mechanisms) that are unstable and can vary across environments. A graph of the DGP in the pneumonia example is given in Fig 1, in which the

\*Much of this work was conducted while at IBM Research AI

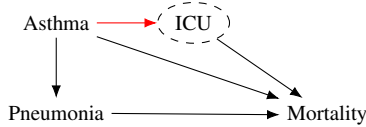


Figure 1: Posited graph for the pneumonia example of Caruana et al. (2015). The red edge represents the unstable relationship while the dashed node represents an unobserved variable.

unstable edge (red) encodes the varying association due to ICU admission policy  $P(I|A)$ . To prevent failures due to anticipated shifts in environment, methods for addressing the shifts seek to find *stable* distributions that are invariant to arbitrary changes in the unstable conditionals. In this case, had ICU status been observed  $P(M|P, A, do(I)) = P(M|P, A, I)$  is a stable distribution that could be used to make mortality predictions that are invariant to differences in ICU admission policy (Schulam and Saria, 2017; Subbaswamy et al., 2019).

These shifts happen in nearly every domain where machine learning is deployed, since the data were generated or collected according to some process. The importance of the explicit graphical representation of the DGP is to allow us to identify and express the pieces of the DGP we want to guard against shifts.<sup>2</sup> However, in broader contexts than reliability, prior work has considered the problem of making invariant predictions that generalize to new, unseen environments, with a number of methods using heterogeneous data from multiple source environments to empirically find stable distributions which are invariant to the shifts (Peters et al., 2016; Rojas-Carulla et al., 2018; Magliacane et al., 2018; Kuang et al., 2018). Additionally, other work has considered specific types of shifts, such as mean-shifts in mechanisms (Rothenhäusler et al., 2018) or shifts in edge strengths (Subbaswamy and Saria, 2018).

While these various methods all find stable distributions, we will show they do not necessarily find the same ones and that this has performance implications. To understand these implications, we first relate different types of stable distributions in terms of how they correspond to the graph underlying the prediction problem, and extend prior work developing graphical representations of shifts in mechanisms (Pearl and Bareinboim, 2011; Subbaswamy et al., 2019). Through this representation we can analyze the effects of using stable distributions to predict on performance. Relatedly, many works have either demonstrated or proved that when the shifts are arbitrarily strong, an unstable model will perform worse in the target environment than a stable model with respect to *minimax risk*—worst-case expected loss across possible environments. In contrast, we characterize the relative performance of different predictors and provide decision criteria for which predictor should be used.

**Contributions:** In this paper we unify existing work on prediction using stable distributions and analyze the tradeoff between stability and performance. First, we build off previous work to create a general graphical representation for arbitrary-strength shifts of different types in terms of edges in the graph. Second, we use the representation to provide a graphical characterization of stable distributions as distributions which effectively disable or remove unstable edges in the graph. Third, we develop a hierarchy of stable distributions in terms of their expressiveness, making connections to various types of causal distributions and how they differ in their precision in removing unstable edges. Fourth, we investigate the effect of edge deletion on prediction performance in the linear case. We then examine the tradeoff between stability and performance under uncertainty in environments in simulated and real data.

## 2 Related Work

Traditional approaches for addressing dataset shift typically assume access to unlabeled samples from the target distribution, which they use to reweight training data during learning (see, e.g., Quiñero-Candela et al. (2009) for an overview). However, when the target environment is unknown (such as in the context of reliability) we require *proactive* methods that learn without requiring samples from the target environment (Subbaswamy and Saria, 2018). Proactive methods make assumptions about the

<sup>2</sup>In practice, the graph may not be fully known. However, assumptions about full knowledge of the DGP can be relaxed using *structure learning* (Spirtes et al., 2000) methods to learn the graph up to an equivalence class from data. We can then consider sensitivity of solutions across each member of the equivalence class.

set of possible target environments in order to be able to learn a model from source environment data that can be applied elsewhere. In this paper we focus on shifts of arbitrary strengths, though others have considered how to make predictions with *bounded magnitude distributional robustness* (e.g., Sinha et al. (2017); Heinze-Deml and Meinshausen (2017)). Most relevant to this work, Rothenhäusler et al. (2018) consider bounded mean-shifts in mechanisms but show that for unbounded strength mean-shifts the solution reduces to a stable distribution.

Another class of proactive methods is entirely data-driven approaches which use data from multiple source environments. They are motivated by the observation that, assuming there are no shifts to the target prediction variable itself, the distribution of a variable given all of its parents in a causal graph is invariant to arbitrary shifts in all other variables (including its parents). This is known as the “independence of cause and mechanism” (Peters et al., 2017) which, in the case of no unobserved variables, has led to methods for *causal discovery* that empirically determine the causal relationships using data from multiple environments (Peters et al., 2016; Heinze-Deml et al., 2018). Leveraging this for the purposes of invariant prediction, recent works employ similar techniques to find an invariant subset of features  $\mathbf{X}$  that yield a stable conditional distribution  $P(Y|\mathbf{X})$  that can be used to predict (Rojas-Carulla et al., 2018; Magliacane et al., 2018). For settings in which data from only one source environment are available, Kuang et al. (2018) use covariate balancing techniques to determine the causal features that yield a stable conditional.

These methods all make assumptions about types of graphs underlying the data they are applied to, such as assumptions about the existence of unobserved confounders or the existence of a stable feature set. In contrast, other methods assume explicit knowledge of the graph representing the DGP. Given additional knowledge of the mechanisms that are expected to vary across environments, these methods return a stable distribution if it exists. They not only consider conditional distributions, but also interventional (Subbaswamy et al., 2019) and counterfactual distributions (Subbaswamy and Saria, 2018). Notably, Subbaswamy et al. (2019) use *selection diagrams* (Pearl and Bareinboim, 2011) to identify mechanisms that can shift. In section 3 we will develop an edge-based representation for shifts of arbitrary types, that in some cases is more expressive in that it identifies the particular edge in a mechanism that is unstable.

### 3 A Causal Hierarchy of Stable Distributions

We first introduce necessary background on causal graphs before defining stability and the types of shifts in mechanism previously considered. We then develop a common graphical representation for expressing arbitrary-strength shifts of different types, and provide a graphical criterion for determining the stability of a distribution. We relate existing methods for finding stable distributions by placing them in a hierarchy of increasing precision in disabling unstable edges. Motivated by these findings, in Section 4 we will quantify the performance impact associated with disabling edges. Proofs of results are in the supplement.

#### 3.1 Preliminaries

**Notation** Throughout the paper sets of variables are denoted by bold capital letters while their particular assignments are denoted by bold lowercase letters. We will consider graphs with directed or bidirected edges (e.g.,  $\leftrightarrow$ ). Acyclic will be taken to mean that there exists no purely directed cycle. The sets of parents, children, ancestors, and descendants in a graph  $\mathcal{G}$  will be denoted by  $pa_{\mathcal{G}}(\cdot)$ ,  $ch_{\mathcal{G}}(\cdot)$ ,  $an_{\mathcal{G}}(\cdot)$ , and  $de_{\mathcal{G}}(\cdot)$ , respectively (subscript  $\mathcal{G}$  omitted when obvious from context). For an edge  $e$ ,  $He(e)$  and  $Ta(e)$  will refer to the head and tail of the edge, respectively.

**Structural Causal Models** We will represent the data generating process (DGP) underlying a prediction problem using a graph,  $\mathcal{G}$ , which consists of a set of vertices  $\mathbf{O}$  corresponding to observed variables and sets of directed and bidirected edges such that there are no directed cycles. Directed edges indicate direct causal effects while bidirected edges indicate the presence of an unobserved confounder (common cause) of the two variables. The prediction problem associated with the graph consists of a target output variable  $Y$  and the remaining observed variables as input features.

The graph  $\mathcal{G}$  defines a Structural Causal Model (SCM) (Pearl, 2009) in which each variable  $V_i \in \mathbf{O}$  is generated as a function of its parents and its variable-specific exogenous noise variable  $U_i$ :  $V_i = f_i(pa(V_i), U_i)$ . For our performance analysis we will consider linear Gaussian SCMs which

can be expressed as a set of equations  $\mathbf{O} = \Lambda \mathbf{O} + \mathbf{U}$ .  $\Lambda$  can be arranged as a lower triangular matrix of structural coefficients associated with directed edges in  $\mathcal{G}$  and  $\mathbf{U}$  are the multivariate Gaussian distributed exogenous variables with covariance matrix  $\mathcal{E}$ . Nonzero off-diagonal elements of  $\mathcal{E}$  correspond to bidirected edges in  $\mathcal{G}$ . The covariance matrix of linear Gaussian SCMs decomposes as  $\Sigma = (I - \Lambda)^{-\top} \mathcal{E} (I - \Lambda)^{-1}$ , a property we will exploit in our analysis of performance. We will further assume that all variables are mean 0.

### 3.2 Stability and Types of Shifts

In this section we introduce the relevant types of shifts before graphically defining instability in terms of edges. To define the shifts, assume that there is a set of environments such that a prediction problem maps to the same graph structure  $\mathcal{G}$ . However, each environment is a different instantiation of that graph such that certain mechanisms differ. One example was Fig 1, in which the graph was the same in both environments but the ICU admission policy was different. As another simple example, consider the graph in Fig 2a. Suppose we wanted to diagnose pneumonia  $Y$  from chest X-rays  $Z$  and stylistic features (i.e., text, orientation, coloring) of the image  $X$ . The latent variable  $W$  represents the hospital department the patient visited. Because each department has its own protocols and equipment, the style preferences  $P(X|W)$  vary across departments. Since in this case  $W$  is not recorded, a model of  $P(Y|X, Z)$  will learn an association between  $Y$  and  $Z$  through  $W$ , so pneumonia predictions will be unreliable in new departments or when equipment/protocols change. This is a case in which we desire invariance to *arbitrary shifts* in the style mechanism  $P(X|W)$ .

**Definition 1** (Arbitrary shifts in mechanism). An arbitrary shift in the mechanism generating a variable  $V$  corresponds to arbitrary shifts in the distribution  $P(V|pa(V))$ .

This is the most common and general shift considered in prior work (Peters et al., 2016; Rojas-Carulla et al., 2018; Magliacane et al., 2018; Kuang et al., 2018; Subbaswamy et al., 2019). For methods that do not assume the graph is known, they assume there exists a subset of features  $\mathbf{X}$  such that  $P(Y|\mathbf{X})$  is stable to arbitrary shifts in the mechanisms of all variables except  $Y$ . *Mean-shifted mechanisms* are a special case that has also been studied (Meinshausen, 2018; Rothenhäusler et al., 2018).

**Definition 2** (Mean-shifted mechanisms). An (arbitrary) mean-shift in the mechanism generating a variable  $V$  corresponds to an environment-specific (arbitrary) change in the intercept of its linear structural equation  $V = \text{intercept}_{env} + \sum_{X \in pa(V)} \lambda_{xv} X + u_v$ .

Finally, Subbaswamy and Saria (2018) consider another special case: *edge-strength shifts* in which a subset of edges into a variable may vary.

**Definition 3** (Edge-strength shift). An edge-strength shift in edge  $X \rightarrow V$  corresponds to a change in the *natural direct effect*: for  $Y = pa(V) \setminus X$  we have that  $E[V(x', Y(x)) - V(x)]$  changes, where  $V(x)$  is the counterfactual value of  $V$  had  $X$  been  $x$ .

All of these shifts can be expressed in terms of edges. First, edge-strength shifts naturally correspond to particular edges. Next, since the mechanism generating a variable  $V$  is encoded graphically by all of the edges into  $V$ , shifts in mechanism can also be represented by marking all edges into  $V$ .<sup>3</sup> Finally, mean-shifts correspond to an edge  $A \rightarrow V$  where for environment (or “anchor”)  $A$  the mean of  $V$  is shifted. We will denote the set of *unstable edges* that can vary across environments as  $E_u \subseteq E$  where  $E$  is the set of edges in  $\mathcal{G}$ . Graphically, unstable edges will be colored.

**Definition 4** (Unstable Edge). An edge is said to be unstable if it is the target of an edge-strength shift or the mechanism associated with the edge is the target of an arbitrary shift.

We can now define *stable distributions*, which are the target of estimation for the methods addressing instability due to shifts. A *stable predictor* will be a model of a stable distribution.

**Definition 5** (Stable Distribution). A distribution  $P(Y|\mathbf{Z})$  is said to be a stable if for any two environments  $\mathcal{G}_1$  and  $\mathcal{G}_2$  that are instantiations of the same graph  $\mathcal{G}$ ,  $P_{\mathcal{G}_1}(Y|\mathbf{Z}) = P_{\mathcal{G}_2}(Y|\mathbf{Z})$  holds.

Having established a common graphical representation for arbitrary shifts of various types, we now provide a graphical definition of stable distributions. First, define an active *unstable path* to be

<sup>3</sup>For shifts in mechanism to an exogenous variable  $V$  with no parents in the graph, one might imagine adding an explicit mechanism variable  $M_V$  to the graph and considering the edge  $M_V \rightarrow V$  to be unstable.

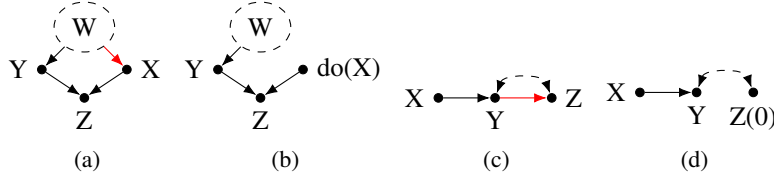


Figure 2: (a-b) Graphs in which a level 2 distribution cannot be expressed as a level 1 distribution. (c-d) Graphs in which a level 3 distribution cannot be expressed as a level 2 distribution. Red denotes an unstable edge.

an active path (as determined by the rules of  $d$ -separation (Pearl, 1988)) that contains at least one unstable edge. The following result tells us that the non-existence of unstable paths is a graphical criterion for determining a distribution’s stability.

**Theorem 1.**  $P(Y|Z)$  is stable if there is no active unstable path from  $Z$  to  $Y$  in  $\mathcal{G}$  and the mechanism generating  $Y$  is stable.

In the next section we use the graphical characterization provided by Thm 1 to differentiate between the types of stable distributions found by existing methods.

### 3.3 The Hierarchy of Stable Distributions

In the previous subsection we established that instability in a graph corresponds to unstable edges, and that stable distributions are those that do not make use of associations containing unstable edges. We now place the types of stable distributions found by existing methods into 3 categories that follow the hierarchy of causal queries (Pearl, 2009, 2018): 1) observational conditionals, 2) conditional interventionals, and 3) counterfactuals. In doing so we show that they differ in the precision with which they can remove edges.

Methods at level 1 of the hierarchy seek invariant conditional distributions of the form  $P(Y|Z)$  that use a subset of observed features for prediction (Peters et al., 2016; Rojas-Carulla et al., 2018; Magliacane et al., 2018; Kuang et al., 2018). These distributions only have conditioning (i.e., the standard rules of  $d$ -separation) as a tool for disabling unstable edges. Methods at level 2 (Subbaswamy et al., 2019) aim for conditional interventional distributions (Pearl, 2009) of the form  $P(Y|do(W), Z)$ . In addition to conditioning, level 2 distributions use the  $do$  operator, which deletes all edges into an intervened variable. Finally, level 3 methods (Subbaswamy and Saria, 2018) seek distributions corresponding to counterfactuals. Counterfactuals allow us to consider conflicting values of a variable. For example, let  $Y$  and  $Z$  denote two children of a variable  $X$ . If we hypothetically set  $X$  to  $x'$  for  $X \rightarrow Y$  but left  $X$  as its observed value  $x$  for  $X \rightarrow Z$ , this corresponds to counterfactual  $Y(x')$  and factual  $Z(x) = Z$ . The importance of counterfactuals is that by setting a variable to a reference value (e.g., 0) for one edge but not others we are effectively removing that single edge.

**Lemma 2.** A stable level 1 distribution of the form  $P(Y|Z)$  can be expressed as a stable level 2 distribution of the form  $P(Y|Z', do(W))$  for  $Z' \subseteq Z \subseteq O$ ,  $W \subseteq O$ .

**Lemma 3.** A stable level 2 distribution of the form  $P(Y|Z', do(W))$  can be expressed as a stable level 3 distribution of the form  $P(Y(W)|Z'(W))$ .

The previous two results capture that stable level 1 distributions are expressible as stable level 2 distributions, which are themselves expressible as stable level 3 distributions. We will now show that higher level distributions in the hierarchy have increased precision in removing individual edges. To witness that the converse of Lemma 2 does not hold, consider the graphs in Fig 2(a-b) with prediction target  $Y$ . The only stable level 1 distribution in (a) is  $P(Y)$  since conditioning on  $X$  or  $Z$  activates the path through the unstable (red) edge. However,  $P(Y|do(X), Z)$  is a stable level 2 distribution (in (b) the unstable edge is deleted). Thus, while the stable level 1 distribution removes all edges in the graph, the level 2 distribution only removed the unstable edge. Similarly, to witness that the converse of Lemma 3 does not hold consider the graphs in Fig 2(c-d). In (c), the level 2 distribution  $P(Y|X, do(Z)) = P(Y|X)$  is stable but it deletes both the unstable  $Y \rightarrow Z$  edge and the stable  $Y \leftrightarrow Z$  edge. However, the counterfactual level 3 distribution  $P(Y|X, Z(Y = 0))$  is stable and only removes the unstable edge (as shown in (d)). The following corollary is now immediate:

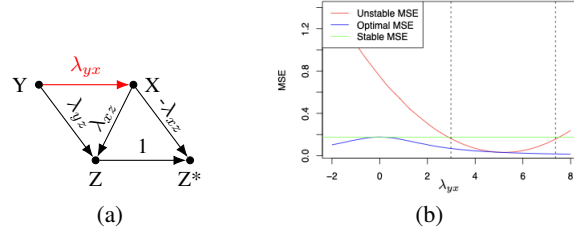


Figure 3: (a) Example with the AV  $Z^*$ .  $P(Y|Z^*)$  is the optimal stable level 3 distribution. (b) Oracle and stable MSEs as  $\lambda_{yx}$  varies.

**Corollary 4.** *Distributions at increasing levels of the hierarchy of stability grant increased precision in disabling individual edges (and thus paths).*

Thus, the difference between stable distributions is their ability to delete edges into a variable in addition to conditioning: level 1 cannot delete edges into a variable, level 2 deletes all edges into a variable, and level 3 can precisely delete a single edge into a variable.<sup>4</sup> The relevant question for their use in practice, then, is how does the removal of edges affect prediction performance? We investigate this in the next section.

## 4 On the Performance of Stable Distributions

In the previous subsection we established that methods for stable prediction achieve stability through hypothetical deletions of edges in the graph underlying a prediction problem. In this section we wish to understand how edge deletion affects performance. To facilitate the analysis, we will consider linear SCMs and quantify how far a stable distribution is from achieving the highest achievable performance in a given environment. Note that in any given environment the optimal predictor (w.r.t. mean squared error (MSE)) is the conditional expectation  $E[Y|\mathbf{O}]$  (Friedman et al., 2001). Thus, we will define the *regret* associated with a given environment to be the difference in performance between a stable predictor and the *oracle* conditional expectation in that environment.

We will consider the form of a level 3 stable distribution since they generalize all stable distributions (Lemma 3) and have the greatest precision in removing singular edges (Corollary 4):  $P(Y|\mathbf{W}^*, \mathbf{Z})$ , where  $\mathbf{Z} \subseteq \mathbf{O}$  consists of observed variables and  $\mathbf{W}^* \cap \mathbf{O} = \emptyset$  consists of counterfactual versions of observed variables (Subbaswamy and Saria, 2018). Interestingly, this means the only difference between a level 3 stable predictor ( $E[Y|\mathbf{W}^*, \mathbf{Z}]$ ) and an oracle predictor is the feature set. Thus, regret reduces to a difference in performance attributable to the oracle’s use of  $\mathbf{X} = \mathbf{O} \setminus (\mathbf{Z} \cup \mathbf{W})$ . Note that in the linear case, counterfactuals take the form of *auxiliary variables* (AVs) (Chen et al., 2016, 2017): modifications of observed variables in which the effects of some (or all) observed parents are removed. For example, in Fig 3a we have the AV  $Z^* = Z - \lambda_{xz}X$  which subtracts out the effect of  $X$  on  $Z$ . With respect to  $Z^*$ , the edge  $X \rightarrow Z$  is effectively removed. Thus,  $P(Y|Z^*)$  is the optimal stable predictor since any additional conditioning would activate unstable edge  $\lambda_{yx}$ .

**Theorem 5.** *For mean zero linear Gaussian SCMs, the MSE of a stable predictor is constant across environments.*

**Theorem 6.** *Let  $\mathcal{G}_0$  be the environment in which the coefficients associated with the unstable edges  $E_u$  are all zero. In  $\mathcal{G}_0$ , the MSE of the oracle predictor  $E_{\mathcal{G}_0}[Y|\mathbf{O}]$  is equal to the MSE of the optimal stable predictor  $E_{\mathcal{G}_0}[Y|\mathbf{Z}, \mathbf{W}^*]$ .*

We have established when the stable MSE is equal to the oracle MSE and that the performance of a stable predictor is a constant baseline across environments. The next result identifies environments for which the oracle MSE is lowest (and thus maximally different from the stable MSE).

<sup>4</sup>We note that the increasing precision at higher levels of the hierarchy does come at a cost: the higher level distributions cannot always be estimated from observational training data. Further, estimation of counterfactuals requires assumptions (additional to those required for level 2) about the functional form of the SCM. As these conditions are not the focus of the current work, for the *identification* conditions required to estimate stable level 2 and level 3 distributions we refer readers to Subbaswamy et al. (2019) and Subbaswamy and Saria (2018).

**Lemma 7.** *Suppose there is only one unstable edge  $e$  with corresponding coefficient  $\lambda$  and that this edge is active for the oracle predictor. As  $|\lambda| \rightarrow \infty$  we have that the oracle MSE  $\rightarrow 0$ .*

To visualize these results in the context of example Fig 3a, in Fig 3b we plot the MSE of the oracle predictor  $E[Y|X, Z]$  (blue) and stable predictor  $E[Y|Z^*]$  (green) as we vary the strength of the unstable edge  $\lambda_{yx}$ . As we expect, the gap between the stable and oracle MSEs increases with the strength of the unstable edge. As a result, we lose the most information when the unstable association is strongest. There is also an implication for the training of unstable predictors: for source environments with smaller unstable edge strengths, an unstable predictor will be less sensitive to changes than if it were trained in an environment with a strong unstable association.

## 5 Trading Off Stability vs Performance Under Uncertainty

### 5.1 Choosing to Reincorporate Unstable Edges

---

**Algorithm 1:** Stepwise Instability Reincorporation

---

**input :** Prior  $P(\theta)$ , Features  $\mathbf{W}^* \cup \mathbf{Z}$ , Remaining features  $\mathbf{X}$ , Covariance  $\Sigma(\theta)$

**output :** New feature set

**F** =  $\mathbf{W}^* \cup \mathbf{Z}$ ; **while**  $\mathbf{X} \neq \emptyset$  *and adding features to F lowers  $\hat{E}_{P(\theta)}[MSE]$*  **do**

    Find  $X \in \mathbf{X}$  that most lowers  $\hat{E}_{P(\theta)}[MSE]$ ;

**F** =  $\mathbf{F} \cup \{X\}$ ;  $\mathbf{X} = \mathbf{X} \setminus \{X\}$ ;

**return** **F**,  $\beta_{Y, \mathbf{F}}$

---

We have just seen that deleting edges incurs performance regret in nearly every environment. This is the consequence of minimizing worst-case (minimax) loss (Berger, 2013), in which case the constant performance of a stable predictor is optimal. However, consider the MSE of an unstable predictor (red) in Fig 3b. From this we see that for finite deviations (interval between the dashed lines) from the source environment ( $\lambda_{yx} = 5$ ) an unstable predictor is preferable to a stable one. Thus, given a stable predictor we might consider: should we reincorporate any unstable edges on the basis of environments we expect to see?

Since there exists a set of environments for which an unstable predictor is preferable, a user might specify a subjective prior over possible environments  $P(\theta)$  and seek to reinclude unstable edges that minimize the expected risk across probable environments:  $E_\theta[MSE]$ . Given two sets of regression weights  $\beta_1, \beta_2$  (e.g., one corresponding to a stable predictor), we could choose between them by Monte Carlo sampling possible environments and computing the average MSE using Eq 1, where  $e_y$  is a one-hot vector and the target environment’s covariance matrix is  $\Sigma = \Sigma(\theta)$ :

$$MSE(\beta) = E[(Y - \hat{Y})^2] = e_y^\top \Sigma e_y - 2\beta^\top \Sigma e_y + \beta^\top \Sigma \beta \quad (1)$$

We could use this to consider adding unstable associations back into a stable predictor in a stepwise fashion (Alg 1). Recalling that in addition to the features used by a level 3 stable predictor ( $E[Y|\mathbf{W}^*, \mathbf{Z}]$ ), an oracle predictor uses factual variables  $\mathbf{X} = \mathbf{O} \setminus (\mathbf{Z} \cup \mathbf{W})$ , we can consider reincorporating them into the feature set so long as they reduce the expected risk. We demonstrate this algorithm in a simulated experiment that shows how adding unstable edges results in a tradeoff between average regret across environments and worst-case loss.

### 5.2 Simulated Experiment

Using the example from Fig 3a, we demonstrate how varying uncertainty in target environment affects 1) the decision to reinclude unstable associations on the basis of average performance and 2) the corresponding affect on worst-case loss. We posit a normal prior over the unstable edge coefficient centered at its source environment value and consider what happens as we increase the prior’s standard deviation  $\sigma$ , representing less certainty in the similarity of possible environments. We apply Algorithm 1 and compare the average regret and worst-case MSE associated with stable, unstable, and stepwise unstable predictors as assessed by 1000 samples from each prior.

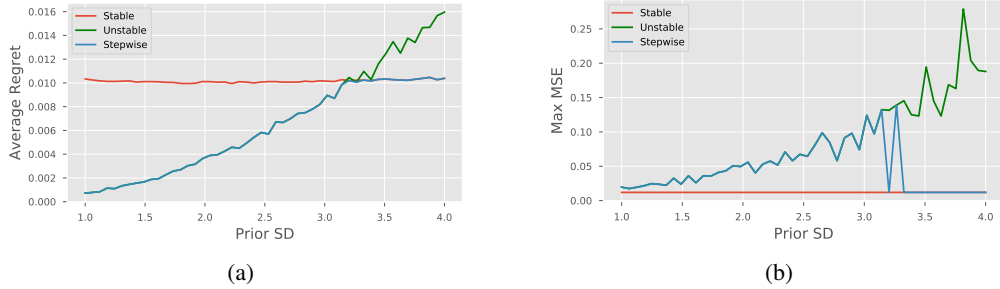


Figure 4: (a) Average regret and (b) minimax MSE for increasingly diffuse priors over environments.

The results (plotted in Fig 4) demonstrate a clear tradeoff between local (average regret) and global (minimax MSE) performance. While for the bottom 66% of the priors ( $\sigma < 3.1$ ) the unstable predictor has lower average regret, it has a worse max MSE for all priors considered. The stepwise predictor produced by Alg 1 uses a decision rule that only considers average performance. As we expect, we see that the stepwise predictor results in the unstable predictor for priors in which the unstable predictor has lower average regret. More generally, this experiment shows that the optimality of stable predictors is closely tied to the choice of performance metric and degree of uncertainty. When we are concerned about the worst-case or when there is high variability in the possible environments, using only stable information to predict will be preferable. For other cases this motivates future work on how to optimally incorporate unstable associations.

### 5.3 Quantifying Instability in Real Data

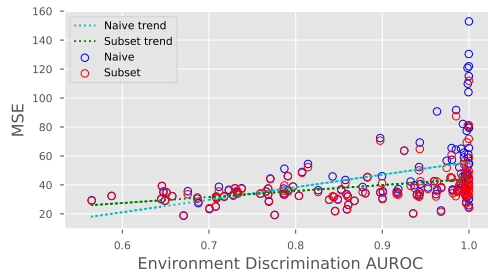


Figure 5: MSEs of a regression using all features (blue pts) vs a invariance-driven subset (vars except temp; red pts) in environments (defined by month) of varying similarity to the source environment.

We now turn to a real data example to examine the degree to which our performance analysis results can extend to complex scenarios and demonstrate challenges that remain in conducting performance analysis beyond the linear case. We use the UCI Bike Sharing dataset (Fanaee-T and Gama, 2013) which has been previously used to investigate shifts in environment (Rothenhäusler et al., 2018; Subbaswamy et al., 2019). It contains 2 years of weather data features (temperature, feeling temperature, wind speed, and humidity) to be used for predicting the number of hourly bike rentals. To define different environments we split the data by month such that the environments will vary in weather patterns and bike rental habits. Application of our analysis is challenging: the data are nonlinear (target variable is square root of rental numbers) and the graph is unknown. Further, it is reasonable to assume that the mechanism that determines bike rentals (our target) itself varies across environments. To test this, however, we used a data-driven method (Rojas-Carulla et al., 2018) on held-out data to search for invariant feature subsets.<sup>5</sup>

We took each month as the source environment and evaluated on the other 11 environments, measuring performance in terms of the MSE of linear regressions with different feature subsets returned by the algorithm. To quantify possible shifts between environments, for each (source, target) pair we

<sup>5</sup>Experimental details, nonlinear regressors, and further discussion in the supplement.



trained a logistic regression to distinguish between the environments and used the resulting area under the ROC curve (AUROC). Values close to 1 indicate easy discrimination and thus more significant shifts. We plot a comparison of two feature subsets in Fig 5 (full feature set vs when temperature is removed). As expected, performance becomes worse and highly varying when the environment pairs are most distinguishable. This corresponds with our findings in section 5.1 and Fig 3b. Contrary to our findings, both feature sets have similar performances in the source environments (both have an average source MSE of 29). In this case the smaller feature set is strictly preferable and does not demonstrate a performance tradeoff for its (relative) stability. Further, it is difficult to attribute reduced variance in the feature subset’s performance to more stability because unstable associations, model misspecification (incorrect weights will lead to instability in Eq 1), and shifts in the target variable (no stable distribution exists) will all contribute to unstable performance. For this reason, future tools for disentangling sources of instability could help to debug highly variant performance.

## 6 Conclusion

The use of machine learning in production represents a shift from applying models to datasets to applying them in the real world. As a result, aspects of the underlying DGP are almost certain to change. Both theoretically and in practice it has been shown that ignoring such shifts can lead to much worse performance upon deployment, and more importantly to unsafe decisions (Schulam and Saria, 2017; Zech et al., 2018). To better characterize this problem, we developed a framework for expressing various types of shifts as unstable edges in a graph, and connected existing stable solutions for addressing the problem to edge deletion. We also showed that interventional and counterfactual distributions are the most precise in deleting edges. However, these types of distribution are not commonly used for prediction today due to complications related to the assumptions required for their estimation. As a result, it is difficult to develop estimators that only remove the necessary edges, and this remains an open problem. Regarding performance, we showed that deleting edges induces regret related to the strength of the removed associations. On average this can lead to worse performance across environments and in cases when variability in environments is low. Future work may more closely examine how to balance between worst-case performance and expected performance.

## References

- Dario Amodei, Chris Olah, Jacob Steinhardt, Paul Christiano, John Schulman, and Dan Mané. Concrete problems in ai safety. *arXiv preprint arXiv:1606.06565*, 2016.
- James O Berger. *Statistical decision theory and Bayesian analysis*. Springer Science & Business Media, 2013.
- Rich Caruana, Yin Lou, Johannes Gehrke, Paul Koch, Marc Sturm, and Noemie Elhadad. Intelligible models for healthcare: Predicting pneumonia risk and hospital 30-day readmission. In *Proceedings of the 21th ACM SIGKDD International Conference on Knowledge Discovery and Data Mining*, pages 1721–1730. ACM, 2015.
- Bryant Chen, Judea Pearl, and Elias Bareinboim. Incorporating knowledge into structural equation models using auxiliary variables. In *Proceedings of the Twenty-Fifth International Joint Conference on Artificial Intelligence*, pages 3577–3583. AAAI Press, 2016.
- Bryant Chen, Daniel Kumor, and Elias Bareinboim. Identification and model testing in linear structural equation models using auxiliary variables. In *Proceedings of the 34th International Conference on Machine Learning-Volume 70*, pages 757–766. JMLR. org, 2017.
- Gregory F Cooper, Constantin F Aliferis, Richard Ambrosino, John Aronis, Bruce G Buchanan, Richard Caruana, Michael J Fine, Clark Glymour, Geoffrey Gordon, Barbara H Hanusa, et al. An evaluation of machine-learning methods for predicting pneumonia mortality. *Artificial intelligence in medicine*, 9(2):107–138, 1997.
- Hadi Fanaee-T and Joao Gama. Event labeling combining ensemble detectors and background knowledge. *Progress in Artificial Intelligence*, pages 1–15, 2013.
- Jerome Friedman, Trevor Hastie, and Robert Tibshirani. *The elements of statistical learning*, volume 1. Springer series in statistics New York, 2001.

- Christina Heinze-Deml and Nicolai Meinshausen. Conditional variance penalties and domain shift robustness. *arXiv preprint arXiv:1710.11469*, 2017.
- Christina Heinze-Deml, Jonas Peters, and Nicolai Meinshausen. Invariant causal prediction for nonlinear models. *Journal of Causal Inference*, 6(2), 2018.
- Katharine E Henry, David N Hager, Peter J Pronovost, and Suchi Saria. A targeted real-time early warning score (trewscore) for septic shock. *Science translational medicine*, 7(299):299ra122–299ra122, 2015.
- Kun Kuang, Peng Cui, Susan Athey, Ruoxuan Xiong, and Bo Li. Stable prediction across unknown environments. In *Proceedings of the 24th ACM SIGKDD International Conference on Knowledge Discovery & Data Mining*, pages 1617–1626. ACM, 2018.
- Kristian Lum and William Isaac. To predict and serve? *Significance*, 13(5):14–19, 2016.
- Sara Magliacane, Thijs van Ommen, Tom Claassen, Stephan Bongers, Philip Versteeg, and Joris M Mooij. Domain adaptation by using causal inference to predict invariant conditional distributions. In *Advances in Neural Information Processing Systems*, pages 10869–10879, 2018.
- Nicolai Meinshausen. Causality from a distributional robustness point of view. In *2018 IEEE Data Science Workshop (DSW)*, pages 6–10. IEEE, 2018.
- Judea Pearl. *Probabilistic Reasoning in Intelligent Systems: Networks of Plausible Inference*. Morgan Kaufmann, 1988.
- Judea Pearl. *Causality*. Cambridge university press, 2009.
- Judea Pearl. Theoretical impediments to machine learning with seven sparks from the causal revolution. *arXiv preprint arXiv:1801.04016*, 2018.
- Judea Pearl and Elias Bareinboim. Transportability of causal and statistical relations: a formal approach. In *Proceedings of the Twenty-Fifth AAAI Conference on Artificial Intelligence*, pages 247–254. AAAI Press, 2011.
- Jonas Peters, Peter Bühlmann, and Nicolai Meinshausen. Causal inference by using invariant prediction: identification and confidence intervals. *Journal of the Royal Statistical Society: Series B (Statistical Methodology)*, 78(5):947–1012, 2016.
- Jonas Peters, Dominik Janzing, and Bernhard Schölkopf. *Elements of causal inference: foundations and learning algorithms*. MIT press, 2017.
- J Quiñero-Candela, Masashi Sugiyama, Anton Schwaighofer, and Neil D Lawrence. Dataset shift in machine learning, 2009.
- Mateo Rojas-Carulla, Bernhard Schölkopf, Richard Turner, and Jonas Peters. Invariant models for causal transfer learning. *The Journal of Machine Learning Research*, 19(1):1309–1342, 2018.
- Dominik Rothenhäusler, Nicolai Meinshausen, Peter Bühlmann, and Jonas Peters. Anchor regression: heterogeneous data meets causality. *arXiv preprint arXiv:1801.06229*, 2018.
- Suchi Saria and Adarsh Subbaswamy. Tutorial: Safe and reliable machine learning. In *ACM Conference on Fairness, Accountability, and Transparency (FAT\*)*. ACM, 2019.
- Peter Schulam and Suchi Saria. Reliable decision support using counterfactual models. In *Advances in Neural Information Processing Systems*, pages 1697–1708, 2017.
- Aman Sinha, Hongseok Namkoong, and John Duchi. Certifying some distributional robustness with principled adversarial training. *arXiv preprint arXiv:1710.10571*, 2017.
- Peter Spirtes, Clark N Glymour, Richard Scheines, David Heckerman, Christopher Meek, Gregory Cooper, and Thomas Richardson. *Causation, prediction, and search*. MIT press, 2000.
- Adarsh Subbaswamy and Suchi Saria. Counterfactual normalization: Proactively addressing dataset shift using causal mechanisms. In *Uncertainty in Artificial Intelligence*, 2018.

- Adarsh Subbaswamy, Peter Schulam, and Suchi Saria. Preventing failures due to dataset shift: Learning predictive models that transport. In *Artificial Intelligence and Statistics (AISTATS)*, 2019.
- Kun-Hsing Yu, Andrew L Beam, and Isaac S Kohane. Artificial intelligence in healthcare. *Nature biomedical engineering*, 2(10):719, 2018.
- John R Zech, Marcus A Badgeley, Manway Liu, Anthony B Costa, Joseph J Titano, and Eric Karl Oermann. Variable generalization performance of a deep learning model to detect pneumonia in chest radiographs: A cross-sectional study. *PLoS medicine*, 15(11):e1002683, 2018.

## A Proofs

**Theorem 1.**  $P(Y|\mathbf{Z})$  is stable if there is no active unstable path from  $\mathbf{Z}$  to  $Y$  in  $\mathcal{G}$  and the mechanism generating  $Y$  is stable.

*Proof.* We first translate our unstable edge representation of the graph to the more general selection diagram (Pearl and Bareinboim, 2011) representation used by Subbaswamy et al. (2019). For an edge  $e$  let  $He(e)$  denote the variables that  $e$  points into. Now for each  $e \in \bar{E}_u$ , add a unique selection variable that points to each  $V = He(e)$ . This indicates that the mechanism that generates  $V$  is unstable. From Definition 3 in Subbaswamy et al. (2019) we know that a distribution is stable if  $\mathbf{S} \perp\!\!\!\perp Y$ .

There are two possible ways there can be an active path from a variable  $S \in \mathbf{S}$  to  $Y$ . If there is an active forward path from  $S$  to  $Y$  (e.g.,  $S \rightarrow ch(S) \rightarrow \dots Y$ ) then there is a corresponding active path from  $Ta(e)$  to  $Y$  that contains the unstable edge  $e$  (e.g.,  $Ta(e) - e \rightarrow ch(S) \rightarrow \dots Y$ ). An active forward path can also indicate that the mechanism that generates  $Y$  is unstable.

Alternatively, if there is an active collider path from  $S$  to  $Y$  (e.g.,  $S \rightarrow ch(S) \leftarrow \dots Y$ ) then there is a corresponding active path from  $He(e) = ch(S)$  to  $Y$  that contains  $e$  (e.g.,  $Ta(e) - e \rightarrow ch(S) \leftarrow \dots Y$ ). Thus, in the selection diagram representation if  $P(Y|\mathbf{Z})$  is unstable then there is an active unstable path from  $Z \in \mathbf{Z}$  to  $Y$  since it means  $Y \not\perp\!\!\!\perp \mathbf{S}|\mathbf{Z}$ . Taking the contrapositive of this statement proves the theorem.  $\square$

**Lemma 2.** A stable level 1 distribution of the form  $P(Y|\mathbf{Z})$  can be expressed as a stable level 2 distribution of the form  $P(Y|\mathbf{Z}', do(\mathbf{W}))$  for  $\mathbf{Z}' \subseteq \mathbf{Z} \subseteq \mathbf{O}$ ,  $\mathbf{W} \subseteq \mathbf{O}$ .

*Proof.* This is a restatement of Corollary 1 in Subbaswamy et al. (2019).  $\square$

**Lemma 3.** A stable level 2 distribution of the form  $P(Y|\mathbf{Z}', do(\mathbf{W}))$  can be expressed as a stable level 3 distribution of the form  $P(Y(\mathbf{W})|\mathbf{Z}'(\mathbf{W}))$ .

*Proof.* Consider the (level 2) intervention  $do(X) = x$ . For a variable  $V$  letting  $V(x)$  denote the value  $V$  would have taken had  $X$  been set to  $x$  we have that  $P(V(x)) = P(V|do(x))$ . When interventions are consistent (i.e., for  $x \neq x'$  there are no conflicting interventions  $do(X = x)$  and  $do(X = x')$ ) counterfactuals reduce to the *potential responses* of interventions expressible with the *do* operator (Pearl, 2009, Definition 7.1.4).  $\square$

**Theorem 5.** For mean zero linear Gaussian SCMs, the MSE of a stable predictor is constant across environments.

*Proof.* First, recall that for a feature set  $\mathbf{Z}$ , asymptotically (as sample size becomes infinite)  $MSE = E[Var(Y|\mathbf{Z})]$ . We know a stable predictor models a stable distribution of the form  $P(Y|\mathbf{Z}, \mathbf{W}^*)$ , where  $\mathbf{W}^*$  consists of AVs (i.e., counterfactuals). For any two environments  $\mathcal{G}_1, \mathcal{G}_2$  which are instantiations of the graph  $\mathcal{G}$ , stability yields the following:

$$P_1(Y|\mathbf{Z}, \mathbf{W}^*) = P_2(Y|\mathbf{Z}, \mathbf{W}^*) \implies Var_1(Y|\mathbf{Z}, \mathbf{W}^*) = Var_2(Y|\mathbf{Z}, \mathbf{W}^*).$$

Further, for centered multivariate Gaussians (recall we assumed all variables are mean 0)  $Var(Y|\mathbf{X} = \mathbf{x}) = Var(Y|\mathbf{X})$  such that conditional variance is constant for all values of the conditioned variables. Thus,  $MSE = E[Var(Y|\mathbf{Z}, \mathbf{W}^*)] = Var(Y|\mathbf{Z}, \mathbf{W}^*)$  is the same in  $\mathcal{G}_1$  and  $\mathcal{G}_2$ .  $\square$

**Theorem 6.** Let  $\mathcal{G}_0$  be the environment in which the coefficients associated with the unstable edges  $E_u$  are all zero. In  $\mathcal{G}_0$ , the MSE of the oracle predictor  $E_{\mathcal{G}_0}[Y|\mathbf{O}]$  is equal to the MSE of the optimal stable predictor  $E_{\mathcal{G}_0}[Y|\mathbf{Z}, \mathbf{W}^*]$ .

*Proof.* First, note that a coefficient value of zero is equivalent to deleting an edge. If it is a directed edge, it corresponds to a 0 entry in the structural coefficient matrix  $\Lambda$ . If it is a bidirected edge then it corresponds to a 0 entry in the off-diagonal of the covariance matrix  $\mathcal{E}$  of the exogenous variables.

Graphically, the effect of the *do* operator is to delete the edges into the variables that are intervened upon (i.e.,  $do(X)$  corresponds to the graph  $\mathcal{G}_{\bar{X}}$  (Pearl, 2009)). Thus, if we let  $\mathbf{V} \subseteq \mathbf{O}$  be the variables with unstable edges into them, and  $\bar{\mathbf{U}} = \mathbf{O} \setminus \mathbf{V}$ , then the environment  $\mathcal{G}_0$  is exactly an

environment in which  $P_0(Y|\mathbf{O}) = P(Y|\mathbf{U}, do(\mathbf{V}))$ . Next, by Lemma 3 we know the conditional interventional distribution can be equivalently expressed in the form  $P(Y|\mathbf{Z}, \mathbf{W}^*)$ . Since  $P_0(Y|\mathbf{O}) = P(Y|\mathbf{Z}, \mathbf{W}^*)$ , we have that  $Var_0(Y|\mathbf{O}) = Var(Y|\mathbf{Z}, \mathbf{W}^*)$  and thus the MSEs are equal.  $\square$

**Lemma 7.** *Suppose there is only one unstable edge  $e$  with corresponding coefficient  $\lambda$  and that this edge is active for the oracle predictor. As  $|\lambda| \rightarrow \infty$  we have that the oracle MSE  $\rightarrow 0$ .*

*Proof.* Sketch: Reduce this by considering predicting  $Y$  from a single variable  $X$  (transform the graph after marginalizing and conditioning over the other variables). For linear Gaussian SCMs we have that  $E[Y|X]$  is of the form  $aX + b$ . Thus,  $R^2 = \rho_{xy}^2$  and it suffices to show that  $\lim_{|\lambda| \rightarrow \infty} \rho_{xy}^2 = 1$ .  $\square$

## B Simulation Experiment Details

### B.1 Details

We generated the linear SCMs parameters as follows:

```
import numpy as np

lyx = np.random.uniform(2, 4) * (2 * np.random.binomial(1, 0.5) - 1)
lyz = np.random.uniform(0.1, 2) * (2 * np.random.binomial(1, 0.5) - 1)
lxz = np.random.uniform(0.1, 2) * (2 * np.random.binomial(1, 0.5) - 1)
v = 0.1 ** 2
```

where  $v$  is the variance of the exogenous noise variables. We generated 10,000 training data points and considered 50 increments of the prior standard deviation  $\sigma$  from 1 to 4. To estimate the AV  $Z^*$  we used the estimated coefficient  $\hat{\lambda}_{xz}$  learned from training data.

## C Bikesharing Experiment

Following Rothenhäusler et al. (2018) we use the UCI Bike Sharing dataset (Fanaee-T and Gama, 2013) in which the goal is to predict the number of hourly bike rentals  $R$  from weather data including temperature  $T$ , feeling temperature  $F$ , wind speed  $W$ , and humidity  $H$ . As in Rothenhäusler et al. (2018), we transform  $R$  from a count to continuous variable using the square root. The data contains 17,379 examples with temporal information such as season and year.

Subbaswamy et al. (2019) posited the graph in Fig 6, in which all mechanisms except for  $R$  varied. When we applied their estimator to the month-based split it exhibited highly unstable performance which indicates their hypothesized graph or mechanism shift may not hold. Further, based on the unstable performance of all estimators tried, we believe the mechanism that generates the bike rentals  $R$  likely varies across environments. This instability will only be magnified by model misspecification.

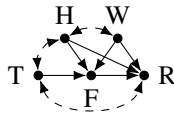


Figure 6: Posited graph from Subbaswamy et al. (2019).

For this reason we turned to Causal transfer learning (CT) Rojas-Carulla et al. (2018) which searches for invariant subsets. The algorithm hyperparameters dictating how much data to use for validation, the significance level, and which hypothesis test to use. In all experiments we set `valid_split = 0.5`, `delta=0.3`, and use `hsic = False` (using HSIC always returned the full feature set). We considered various subsets returned by the algorithm of Rojas-Carulla et al. (2018), the two plotted in the main paper were the subsets which performed the best on a 20% dev holdout. These two subsets were all features and all features except temperature. All other subsets returned exhibited similar behavior. Importantly, all other subsets (that were not all features or all except temperature) exhibited

higher variance in performance and had a higher-sloped trend line than the full feature set. Thus, the two subsets in the main paper had the most stable performance.

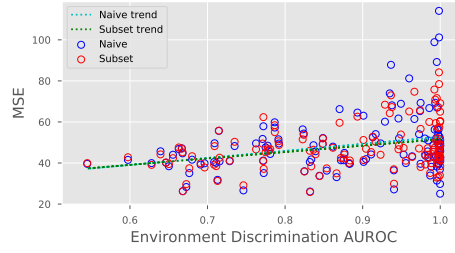


Figure 7: Performance of full and subset (full except temperature) feature sets using random forest regressions.

Given the inherent nonlinearity in the data we additionally tried using random forest regressions (default params in scikit-learn) since this was used in Magliacane et al. (2018) for nonlinear regression with invariant subsets. However, we saw the same trend as in the main paper; see Fig 7 for the performance using random forest regression. In this case it is even clearer that the two feature sets have very similar performance for more similar domains. Additionally, overall the variance in performance is much lower than with the linear regressions, though for significantly shifted target environments (right side of x-axis) there is still higher varying performance (and the full subset still performs worse).